Chinese Chemical Letters 31 (2020) 2725–2729

Contents lists available at ScienceDirect

Chinese Chemical Letters

journal homepage: www.elsevier.com/locate/cclet

Communication

Highly sensitive fluorescence detection of chloride ion in aqueous solution with Ag-modified porous g-C_3N_4 nanosheets

Zishu Zhang[a,b], Ying Gao[a], Peng Li[b,c,**], Binhong Qu[b], Zhiyuan Mu[b], Yang Liu[b], Yang Qu[b], Degui Kong[a], Qing Chang[a,d,***], Liqiang Jing[b,*]

[a] College of Electronic Engineering, Heilongjiang University, Harbin 150080, China
[b] Key Laboratory of Functional Inorganic Materials Chemistry (Ministry of Education), International Joint Research Center for Catalytic Technology, School of Chemistry and Materials Science, Heilongjiang University, Harbin 150080, China
[c] College of Physical Science and Technology, Heilongjiang University, Harbin 150080, China
[d] College of Media Engineering, Communication University of Zhejiang, Hangzhou 310018, China

ARTICLE INFO

Article history:
Received 21 April 2020
Received in revised form 2 May 2020
Accepted 18 May 2020
Available online 26 May 2020

Keywords:
g-C_3N_4
Ag-modification
Chloride ion
Fluorescence detection
Photoinduced charge transfer

ABSTRACT

The porous g-C_3N_4 (PCN) nanosheets are successfully synthesized and further modified with nano-sized Ag by a simple wet-chemical process. Interestingly, the Ag-modified porous g-C_3N_4 (Ag-PCN) nanosheets exhibit competitive fluorescence detection performance of chloride ion (Cl^-) in aqueous solution. Under the optimized conditions, the concentration of Cl^- could be quantitative analyzed with the Ag-PCN in a wide detection range from 0.5 mmol/L to 0.1 mol/L, with a low detection limitation of 0.06 mmol/L. It is confirmed that the fluorescence of PCN could be effectively decayed by the photoinduced charge transfer *via* the adsorbed Cl^- for trapping holes, mainly by means of the time-resolved fluorescence and surface photovoltage spectra. The porous structure and modified Ag promote the adsorption of Cl^- on resulting Ag-PCN, leading to excellent fluorescence detection for Cl^-. This work provides a feasible route to develop a fluorescence detection of Cl^- with g-C_3N_4 nanosheets in environment water.

Chloride ion (Cl^-), as the most common anion, almost exists in environmental water, which is indispensable ion in disinfection and many production processes [1]. Meanwhile, Cl^- plays a role in maintaining the normal function of cells and reacting in the organism [2,3]. Noticeably, the excess Cl^- would easily polarizes and accelerates corrosion reaction of industrial equipment [4]. Importantly, Cl^- can be catalysed and oxidized to produce toxic substances that have carcinogenic effect on human beings and animals [5–7]. Moreover, excess Cl^- of agricultural water would restrain the growth of the crops and causes the soil to acidify and salinization [8]. Therefore, it is necessary to accurate detect the concentration of Cl^- in environmental water.

Several techniques have been employed for the detection and quantification of Cl^-, including colorimetric trituration [9], spectrophotometry [10], ion chromatography [11], ion selective electrode [12], atomic absorption spectrometry [13]. However, the large measurement errors, complex operations, the expensive equipment and long time consuming have limited practical applications of these methods. In comparison with other detection methods, fluorescence detection is a powerful tool due to its simple operation, low amount of detection reagents, non-toxic and high sensitivity. In recent years, some fluorescent materials for detecting Cl^- have been reported [14,15]. However, the complicated synthesis, complex operation, high toxicity and utilization of organic media have limited practical applications of these fluorescent materials for detection of Cl^- in aqueous solutions.

Graphitic carbon nitride (g-C_3N_4) is a new type of promising conjugated polymer semiconductor with suitable energy bandgap, high biocompatibility, good chemical and thermal stability, and unique surface properties [16–18]. Moreover, the g-C_3N_4 can be easily prepared in large scale by condensing nitrogen-rich precursors and exploited into nanosheets [19]. The simple and green synthesis method and excellent characteristics have attracted increasing interest [20] and created potential applications of g-C_3N_4 nanosheets in chemical sensing, utilizing the

* Corresponding author.
** Corresponding author at: Key Laboratory of Functional Inorganic Materials Chemistry (Ministry of Education), International Joint Research Center for Catalytic Technology, School of Chemistry and Materials Science, Heilongjiang University, Harbin 150080, China.
*** Corresponding author at: College of Electronic Engineering, Heilongjiang University, Harbin 150080, China.
E-mail addresses: lipenghit@126.com (P. Li), 15846017711@139.com (Q. Chang), Jinglq@hlju.edu.cn (L. Jing).

https://doi.org/10.1016/j.cclet.2020.05.024
1001-8417/

fluorescence and electrochemiluminescence [21–25]. Utilizing the interactions between the g-C_3N_4 and various targets, many g-C_3N_4 based fluorescent methods have been developed for detecting heavy metal ions [26], inorganic ions [27] and other toxic substances [28]. In our previous works, fluorescent properties of g-C_3N_4 were also investigated to detect chromium ions and TNP in environmental water [29,30]. Therefore, g-C_3N_4 based nanomaterials are very useful for the development of sensitive and label-free fluorescent detection.

Nevertheless, the application of g-C_3N_4 for the fluorescent detection of Cl^- has rarely been explored. Normally, the fluorescence sensitivities of these g-C_3N_4 based nanomaterials are always attributed to the charge transfer and the inner filter effect. The adsorbed Cl^- on the surface of g-C_3N_4 could trap holes so as to facilitate the fluorescence decay of by the charge transfer [31]. Thus, it is conceivable that the g-C_3N_4 may become a promising candidate for fluorescence detection of Cl^-. Importantly, it is meaningful to improve the fluorescence detectability of g-C_3N_4 by promoting the adsorption of Cl^- on g-C_3N_4. Increasing the specific surface areas by introducing porosity into g-C_3N_4 is effective routes to improve the adsorption [32]. Moreover, Ag could easily form complex with Cl^-. It is also possible to use Ag to modify g-C_3N_4 for a better absorbability. To the best of our knowledge, similar modification on g-C_3N_4 for detecting Cl^- has seldom been reported up to now. Thus, it is expected that the fluorescence detectability of g-C_3N_4 for Cl^- can be obviously improved by porous structures and Ag modification.

Based on above discussion, we have synthesized Ag modified porous g-C_3N_4 (Ag-PCN) nanosheets and prepared stable suspension for the fluorescence detection of Cl^- in aqueous solution. It is demonstrated that the modification with Ag could greatly improve the fluorescence detection capacity of porous g-C_3N_4 (PCN) to Cl^-, attributed to the promoted adsorption ability to Cl^-. The fluorescence detection mechanism of Cl^- *via* Ag-PCN has been investigated by the decrease in fluorescence intensity and lifetime. This study provides a novel approach to improve the fluorescence detection performance of g-C_3N_4 for Cl^-, which might serve as an effective method for designing g-C_3N_4-based fluorescent nanomaterials.

The transmission electron microscopy (TEM) was utilized to acquire the features of PCN and Ag-PCN. The PCN with the porous nanosheet structures could be seen in Fig. 1a. Through TEM observation, one can see that Ag-PCN with uniform porous has no distinct morphology changes compared with PCN (Fig. 1b). It may be due to the low amount of loaded Ag on PCN. As shown in Fig. S1a (Supporting information), the estimated BET surface area of PCN is about 54.9 m^2/g, which demonstrates porous structures with the improved adsorption capacity compared with bulk g-C_3N_4. The X-ray diffraction (XRD) patterns of Ag-PCN also show no obvious difference compared to the PCN because of low content of Ag modification (Fig. S1b in Supporting information). Moreover, the diffuse reflectance spectroscopy (DRS) spectra (Fig. 1c) further demonstrate that the energy bandgap of Ag-PCN is almost 2.7 eV, similar to that of PCN. Therefore, it can be concluded that the Ag modification does not change the morphology and crystal phase composition of PCN. The X-ray photoelectron spectroscopy (XPS) measurement was performed to confirm the formation of Ag-PCN composites, and the related Ag 3d XPS spectrum is shown in Fig. 1d. The peaks at 374.8 eV and 368.8 eV in the spectrum of Ag 3d can be directly assigned to the corresponding as Ag $3d_{5/2}$ and Ag $3d_{3/2}$, indicating that there is Ag^0 [33]. Thus, it is deduced that high-dispersion nano-sized metallic Ag exists on PCN. Through the DRS

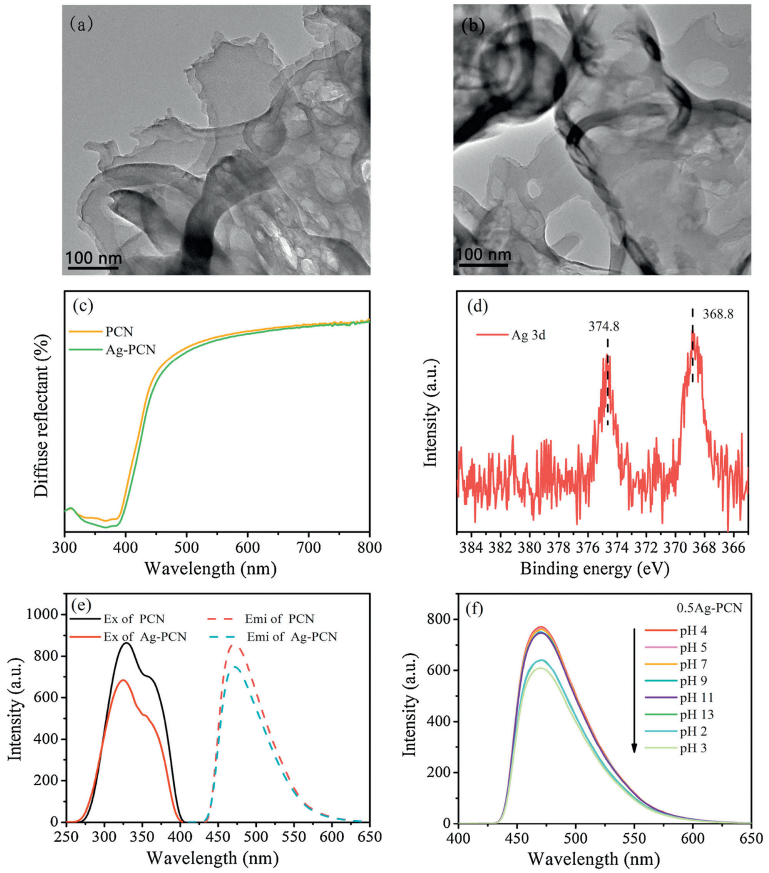

Fig. 1. TEM images of PCN (a) and Ag-PCN (b). (c) DRS spectra of the PCN and Ag-PCN. (d) XPS spectrum of the Ag-PCN. (e) Fluorescence excitation and emission spectra of PCN and Ag-PCN. (f) Effect of different pH on F_0 of Ag-PCN.

and photoluminescence (PL) spectra of PCN and Ag-PCN powders observation in Figs. S2a and b (Supporting information), 0.5Ag-PCN is selected as the optimal-amount Ag-modified one, and is applied in the following fluorescence detection experiments.

Meanwhile, the PCN and 0.5Ag-PCN exhibit good dispersibility and uniformly in the water as shown in Figs. S3a and b (Supporting information). The fluorescence excitation and emission spectra of PCN and Ag-PCN suspensions were further compared to explore the effect of Ag modification on optical properties. The PCN suspension exhibits a maximum emission peak at 470 nm when the excitation wavelength from 290 nm to 350 nm is used, and the strongest emission intensity is located at 325 nm in Fig. 1e. The 0.5Ag-PCN suspension also shows similar emission and excitation peaks positions, with slightly decreased intensity. The relative quantum yield of Ag-PCN can be calculated to be 5.03% by using quinine sulphate as fluorescence reference (Table S1 in the Supporting information). To obtain the optimal conditions for the good fluorescence detection performance of Ag-PCN, the effects of the concentration of Ag-PCN suspension and the pH value on the fluorescence intensity were further analysed. Based on the results in Fig. S3c (Supporting information), it is confirmed that 0.03 g/L is the optimal concentration of Ag-PCN. As shown in Fig. S3d (Supporting information) and Fig. 1f, the fluorescence intensity of PCN and 0.5Ag-PCN remain almost unchanged from pH 4 to pH 11, while obviously decrease under strong acid or alkali conditions.

The fluorescence of PCN/Ag-PCN could be quenched after adsorption of Cl^-, which is related to the pH values of Cl^- solution. The change rate $[(F_0\text{-}F)/F_0]$ of fluorescence intensities of the PCN and Ag-PCN on the conditions of different pH solutions were explored for obtaining the optimal detection performance, and F_0 and F represent the fluorescence intensity in the absence and presence of Cl^-.

In Fig. 2a, it can be seen clearly that the fluorescence intensity of PCN in pH 4 Cl^- solution exhibits the largest change ratio, and slightly decrease from pH 4–10. Meanwhile, Ag-PCN has a similar variation trend. Obviously, the effect of quenching is the best under pH 4 conditions for Cl^- detection. For the fluorescence determination of the PCN and Ag-PCN toward Cl^-, different concentrations of Cl^- in the range of 0.5 mmol/L to 0.1 mol/L were used for detecting under the optimized conditions. As shown in Fig. 2b, the fluorescence intensity gradually decreases with the increase in the amount of added Cl^-. The quenching process could be described by the widely-employed Stern-Volmer equation [34], which is shown as the following Eq. 1:

$$F = \frac{F_0}{1 + K_{sv}[Cl^-]}$$

where K_{sv} is the coefficient of Stern–Volmer plot, $[Cl^-]$ is the concentration of Cl^- in the solution. A good linear correlation between the PCN quenching efficiency and the Cl^- concentration is obtained in the range of 5 mmol/L to 0.1 mol/L with the slope value (K_{sv} = 3.63) under the conditions of pH 4. According to Figs. S4a and b (Supporting information), it also exhibits a certain capacity for detecting Cl^- by utilizing the fluorescence decay of the low concentration PCN or in pH 7. Compared with PCN, Ag-PCN shows obviously superior fluorescence detection for Cl^-. One can see clearly that the fluorescence intensity of 0.5Ag-PCN gradually decreases with increasing the amount of added Cl^- in pH 4 in Fig. 2c. A wider linear relationship between the 0.5Ag-PCN quenching efficiency and the Cl^- concentration is obtained in the range of 0.5 mmol/L to 0.1 mol/L with the slope value (K_{sv} = 8.92),

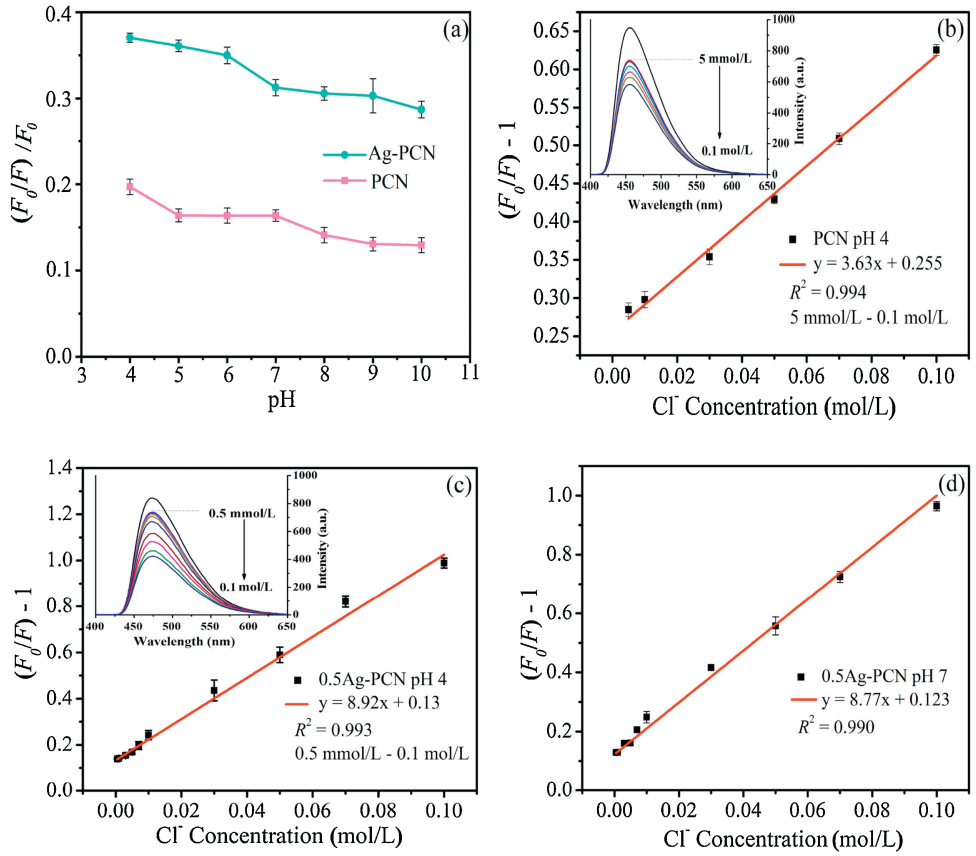

Fig. 2. (a) The fluorescence intensity change ratios $[(F_0\text{-}F)/F_0]$ of the PCN and Ag-PCN in different pH values. Fluorescence determination of Cl^- by PCN in pH 4 (b), Ag-PCN in pH 4 (c), Ag-PCN in pH 7 (d).

which is larger than that of PCN. Under optimal conditions, the limit of detection (LOD) for Cl^- was found to be 0.06 mmol/L, which was comparable with the LODs obtained from other fluorescence methods [15,35]. In addition, the fluorescence determination of Cl^- by Ag-PCN in the neutral condition was also demonstrated. In Fig. 2d, it is shown that the Ag-PCN could also have a good capacity for detecting Cl^- in pH 7 with the slightly lower slope value. To evaluate the selectivity of Cl^-, we employed several anions in the interference experiments including Br^-, F^-, SO_4^{2-}, OH^-, NO_3^-, $C_2O_4^{2-}$ and CH_3COO^- (Fig. S5 in Supporting information). The results demonstrated that these anions hardly affected fluorescence detection [36,37]. These results mean that the as-prepared Ag-PCN exhibits an efficient fluorescence detecting for Cl^-.

On the basis of the above investigations, the fluorescence of PCN could be effectively decayed by adsorbed Cl^-. More importantly, Ag-PCN possesses better fluorescence detection performance for Cl^-, which could be attributed to its strong absorption to Cl^-. In the previous literatures, the conventional fluorescence quenching mechanisms of g-C_3N_4 based nanomaterials are always attributed to the photoinduced electron transfer (PET) or the IFE [38,39]. It is noticed that NaCl has no obvious absorption band over the visible range, and as a result the IFE could not be considered (Fig. S6 in Supporting information). To elucidate the fluorescence decay mechanism of PCN/Ag-PCN toward Cl^-, an atmosphere-controlled steady-state surface photovoltage spectroscopy (SSSPS) is applied to investigate the charge transfer of resultant PCN and Ag-PCN. Fig. S7a (Supporting information) shows that the PCN has a very weak signal, while the SPS response of PCN is significantly enhanced after adsorbing Cl^-, indicating the photogenerated charge transfer and separation happens between PCN and Cl^-. In Fig. S7b (Supporting information), it can be seen clearly that the SPS responses of PCN-Cl is significantly enhanced with the decreased amount of O_2, indicating the enhanced charge separation. Due to the trap electron effect of adsorbing O_2, these results suggest that the adsorbed Cl^- could effectively trap holes so as to make the corresponding electrons preferentially diffuse to the surfaces. Interestingly, one can see that the SPS responses greatly changes under different atmospheric conditions after modifying Ag (Fig. 3a), similar to PCN, which further confirmed the PET effect during the fluorescence quenching of Ag-PCN to Cl^-. For further

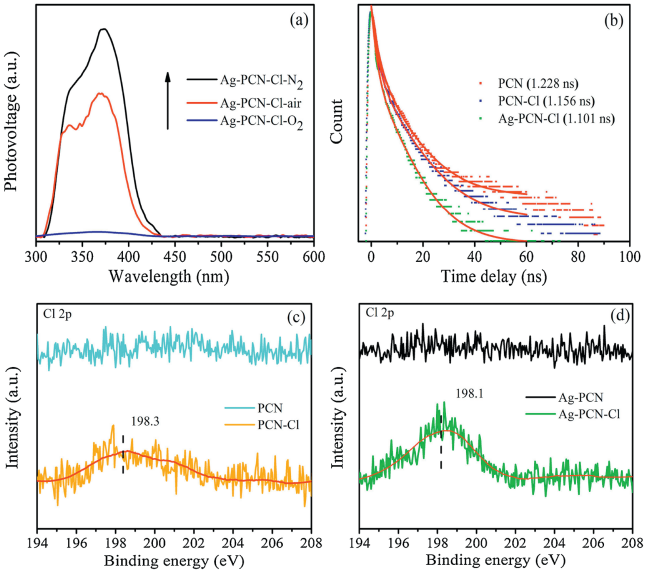

Fig. 3. (a) SPS spectra of Ag-PCN with Cl^- adsorption in N_2, air and O_2. (b) Time-resolved decay of the PCN, PCN and Ag-PCN after adsorbing Cl^-. (c) XPS spectra of the PCN and PCN-Cl. (d) XPS spectra of the Ag-PCN and Ag-PCN-Cl.

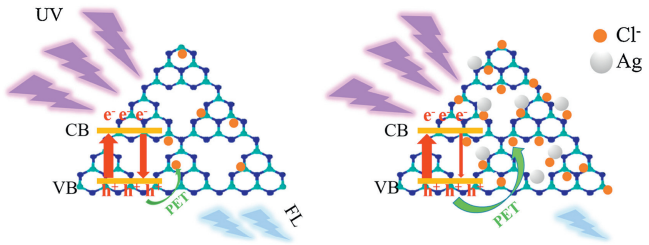

Scheme 1. Schematic of fluorescence detection of Cl^- based on PCN and Ag-PCN.

insights into the effect of Ag modification, the time-resolved fluorescence decay processes of PCN, and Ag-PCN after Cl^- adsorption were recorded. As Fig. 3b shown, a long-time PL decay process for PCN (1.228 ns) is found compared with PCN-Cl (1.156 ns), which is attribute to the efficient PET process so as to make the fluorescence quenching of PCN. Noticeably, the PL decay process for Ag-PCN with Cl^- is the shortest (1.101 ns). The relative standard deviation (RSD) of each fluorescent lifetime measurement was below 1%, revealing the high reproducibility and precision of this approach (Fig. S8 in Supporting information). This further proves that the PET effect is obvious after Ag modification.

To further elucidate the improving detection mechanism of Ag-PCN for Cl^-, Cl 2p XPS spectra were applied to determine the effect of the Ag modification. As shown in Fig. 3c, after absorbing Cl^-, the characteristic peak of Cl 2p at 198.3 eV is obtained [40]. Compared to PCN, the peak position of Ag-PCN is about 198.1 eV, which is basically unchanged but shows a clearly increased effect with Ag modification in Fig. 3d. This is attributed to the more amounts of Cl^- adsorbed on Ag-PCN.

Based on the above comparative investigations, it is confirmed that the improving detection of Cl^- with Ag-PCN is due to its enhanced absorbency for Cl^-. Scheme 1 shows the possible mechanism of fluorescence detection. The PCN emits an obvious blue fluorescence signal under proper light excitation. After adsorbing Cl^-, the fluorescence of PCN is decreased due to the PET process. Meanwhile, the modified Ag on the PCN surface easily forms complex with Cl^- in aqueous solution, leading to more amount of Cl^- adsorption. Thus, the promoted adsorption of Cl^- on PCN is favourable for the PET, so as to increase the fluorescence quenching. As a result, the obtained Ag-PCN could serve as a highly-sensitive fluorescence sensing nanomaterial for detecting Cl^-.

In summary, the Ag-modified porous g-C_3N_4 nanosheets are successfully prepared and used for highly-sensitive fluorescence detection of Cl^- in aqueous solution. The modification with Ag is conducive to adsorb more Cl^- on the resulting Ag-PCN surface, leading to the enhanced PET process by effectively capturing holes with Cl^-. This is well responsible for the obviously-improved fluorescence quenching of Ag-PCN. This present study provides a feasible strategy to improve the fluorescence detection performance of g-C_3N_4 for Cl^- by increasing the adsorption in environment water.

Declaration of competing interest

The authors declare that they have no known competing financial interests or personal relationships that could have appeared to influence the work reported in this paper.

Acknowledgments

The authors are grateful for financial support from the NSFC project (Nos. U1805255, 11704105), Heilongjiang Postdoctoral

Fund (No. LBH-Z17188) and the Fundamental Research Funds of University in Heilongjiang Province (No. 2017-KYYWF-0465).

Appendix A. Supplementary data

Supplementary material related to this article can be found, in the online version, at doi:https://doi.org/10.1016/j.cclet.2020.05.024.

References

[1] N. Winterton, Green Chem. 2 (2000) 173–225.
[2] E.G. Su, R.G. Miche, J. Anal. At. Spectrom. 9 (1994) 501–508.
[3] D. Martin-Yerga, A. Perez-Junquera, M.B. Gonzalez-Garcia, D. Hernandez-Santos, et al., Anal. Chem. 90 (2018) 7442–7449.
[4] N.F. Robaina, F.N. Feiteira, A.R. Cassella, R.J. Cassella, J. Chromatogr. A 1458 (2016) 112–117.
[5] Y. Qin, H.J. Kwon, M.J. Deen, et al., RSC Adv. 5 (2015) 69086–69109.
[6] Y. Dong, G. Li, N. Zhou, et al., Anal. Chem. 84 (2012) 8378–8382.
[7] Y. Yang, J. Shi, Y. Yang, et al., J. Environ. Sci. China 76 (2019) 48–56.
[8] M.A. Wakil, Z.T. Alwahabi, J. Anal. At. Spectrom. 34 (2019) 1892–1899.
[9] M.Y. Kim, E.I. Yang, Constr. Build. Mater. 41 (2013) 239–245.
[10] D.L. Rocha, F.R.P. Rocha, Microchem. J. 108 (2013) 193–197.
[11] C. Lopez-Moreno, I.V. Perez, Food Chem. 194 (2016) 687–694.
[12] P.J. Aruscavage, E.Y. Campbell, Talanta 30 (1983) 745–749.
[13] N.I. Petrova, D.Y. Troitskii, I.I. Novoselov, A.I. Saprykin, Inorg. Mater. Appl. Res. 51 (2015) 559–562.
[14] Y. Ding, J. Ling, J. Cai, et al., Anal. Methods 8 (2016) 1157–1161.
[15] F. Zhang, C. Ma, Y. Wang, et al., Spectrochim. Acta Part A 205 (2018) 428–434.
[16] D. Ni, Y. Shen, S. Liu, et al., Chin. Chem. Lett. 31 (2020) 115–118.
[17] S. Cao, J. Low, J. Yu, M. Jaroniec, Adv. Mater. 27 (2015) 2150–2176.
[18] L. Chen, J. Song, Adv. Funct. Mater. 27 (2017) 1702695.
[19] X. Zhang, X. Xie, B. Pan, et al., J. Am. Chem. Soc. 135 (2013) 18–21.
[20] A. Hatamie, F. Marahel, A. Sharifat, Talanta 76 (2018) 518–525.
[21] S. Feng, P. Yan, L. Xu, et al., Chin. Chem. Lett. 29 (2018) 1629–1632.
[22] X. Zhang, H. Wang, H. Wang, et al., Adv. Mater. 26 (2014) 4438–4443.
[23] Y. Wu, Q. Chen, S. Liu, et al., Chin. Chem. Lett. 30 (2019) 2186–2190.
[24] Q. Liu, D. Zhu, Y. Yu, et al., Chin. Chem. Lett. 30 (2019) 1639–1642.
[25] L. Chen, D. Huang, S. Ren, et al., Nanoscale 5 (2013) 225–230.
[26] J. Tian, Q. Liu, X. Sun, et al., Anal. Chem. 85 (2013) 5595–5599.
[27] Y. Tang, H. Song, Y. Su, Y. Lv, Anal. Chem. 85 (2013) 11876–11884.
[28] J. Chen, Q. Ma, C. Wang, et al., New J. Chem. 41 (2017) 7171–7176.
[29] Y. Liu, Z. Li, P. Li, et al., Mater. Res. Bull. 112 (2019) 9–15.
[30] B. Qu, Z. Mu, Y. Liu, et al., Environ. Sci. Nano 7 (2020) 262–271.
[31] J. Li, X. Zhang, C. Liu, et al., Appl. Catal. B 218 (2017) 60–67.
[32] Y. Chen, Z. Zhan, J. Wang, et al., Chin. Chem. Lett. 29 (2018) 437–440.
[33] Y. Chen, D. He, Y. Situ, et al., ACS Appl. Mater. Interfaces 6 (2014) 14405–14414.
[34] J. Wang, Y. Song, X. Wu, et al., Measurement 46 (2013) 3982–3987.
[35] A. Graefe, S.E. Stanca, S. Nietzsche, L. Kubicova, Anal. Chem. 80 (2008) 6526–6531.
[36] A. Yu, W. Liu, J. Gao, et al., Spectrochim. Acta Part A 233 (2020) 118218.
[37] M. Hong, A. Liu, Y. Xu, et al., Chin. Chem. Lett. 27 (2016) 989–992.
[38] X. Guo, G. Yue, C. Liu, et al., ACS Appl. Mater. Interfaces 10 (2018) 26118–26127.
[39] Z. Guo, B. Li, Y. Zhang, et al., ChemistrySelect 4 (2019) 8178–8182.
[40] H. Xu, L. Zhang, J. Phys. Chem. C 114 (2010) 11534–11541.